

Reversible Gelation in Semidilute Aqueous Solutions of Associative Polymers: A Small-Angle Neutron Scattering Study

Paul D. T. Huibers,[†] Lev E. Bromberg,[†] Brian H. Robinson,[‡] and T. Alan Hatton^{*,†}

Department of Chemical Engineering, Massachusetts Institute of Technology, Cambridge, Massachusetts 02139-4307, and School of Chemical Sciences, University of East Anglia, Norwich NR4 7TJ, United Kingdom

Received February 9, 1999; Revised Manuscript Received May 20, 1999

ABSTRACT: Thermally reversible gelation in 1% aqueous solutions of poly(ethylene oxide)-*b*-poly(propylene oxide)-*b*-poly(ethylene oxide)-*g*-poly(sodium acrylate) has been observed. The transition that occurs as the temperature is increased through the gelation threshold (T_{gel}) is clearly observable by rheological and small-angle neutron scattering (SANS) measurements. SANS measurements suggest that within the hydrogel there exists an unusually uniform matrix of scattering centers, attributed to close packing of micelle-like aggregates surrounded by highly hydrated poly(sodium acrylate) and unassociated ethylene oxide/propylene oxide copolymer. The physical cross-linking caused by these scattering centers induces gelation. Direct model fits to the SANS data suggest that the scattering centers are similar in structure, but somewhat smaller than micelles of the poly(ethylene oxide)-*b*-poly(propylene oxide)-*b*-poly(ethylene oxide) component, with a dehydrated poly(propylene oxide) core of radius 30 Å surrounded by a hydrated PEO corona of outer radius 60 Å.

Introduction

The polymer formed from grafting the branched polyelectrolyte poly(sodium acrylate) (PAA) to the surface-active triblock copolymer poly(ethylene oxide)-*b*-poly(propylene oxide)-*b*-poly(ethylene oxide) (PEO-PPO-PEO) represents a class of unique new materials that undergo reversible gelation in semidilute (1 wt % and below) aqueous solutions over a narrow temperature range.^{1–11} The covalent grafting via C–C bonding results in high molecular weight (above 10⁵ Da) PEO-PPO-PEO-*g*-PAA polymers with regular short-chain branching.⁹ Numerous applications of these polymers, primarily medicinal, stem from their useful thermogelling properties, their benign, nonirritating nature, and their bioadhesive properties.^{1–4,6} Onset of gelation in Pluronic-PAA solutions coincides with the critical micellization temperature (cmt) of the parent Pluronic, where the cmt is defined as the minimum temperature at which micelles start to form from monomer in solution.¹² To date, the role played by the Pluronic moieties in the gelling process has not been identified clearly, nor has the structure of the gels been elucidated, and it is the purpose of this paper to develop some understanding of these issues.

Small-angle neutron scattering (SANS) is a powerful technique to probe the structure of colloidal dispersions, as well as microdomains in polymer solutions and gels (for an extensive review, see ref 13). The short effective wavelength (6 Å) of the neutrons permits the characterization of features with dimensions of the order 5–500 Å. The model for the scattering intensity vs scattering angle [$I(q) \propto NP(q)S(q)$] has three primary components: N , the number density of scattering centers, $P(q)$, the form factor, and $S(q)$, the structure factor; $q = (4\pi/\lambda)\sin \theta$ is the scattering vector for scattering angle θ and wavelength λ . P is a function of the size

and shape of a discrete scattering object, and S describes interparticle interactions. For dilute solutions of dispersed colloids, conditions can often be found where interparticle interactions are insignificant, such that S approaches unity. The scattering measurement then allows an estimation of the form factor, and thus particle size and shape, directly. Many form factors for well-defined particle geometries are available as closed expressions that can be readily solved. For network gels, on the other hand, there is often no true scattering center, and structure factor effects, which capture the interactions in the material related to the cage (network) dimensions, dominate scattering. In addition to scattering from local heterogeneities due to polymer cross-linking and other network effects, long-range polymer concentration fluctuations can also contribute to scattering. These influences on the structure factor are often quite difficult to model in closed form. Thus, the standard procedures of analysis cannot simply be applied.¹³

Bulk gels can be quite amorphous, and a distinct scattering peak in the SANS profiles will only appear if some significant spatial correlation exists. Hydrogels based on cross-linked water-soluble polymers such as poly(vinyl alcohol) have been studied and give scattering profiles without any obvious peaks.^{14–16} Similar results have been obtained for agarose gels.¹⁷ SANS profiles with broad peaks can, however, be obtained from gels of lactoglobulin protein¹⁸ and poly(*N*-isopropylacrylamide) (pNIPA),¹⁹ indicating distinct scattering centers with some degree of order to the spacing between centers. These peaks become more defined for gels from partially charged polymers such as pNIPA-PAA,^{20,21} indicating increased order in the scattering center spacing induced by the presence of a polyelectrolyte component in the polymer.

In this work, we show that SANS measurements of Pluronic-PAA solutions suggest that gelation is coincident with the formation of close-packed scattering centers similar to micelle-like aggregates with hydro-

[†] Massachusetts Institute of Technology.

[‡] University of East Anglia.

* To whom correspondence should be addressed.

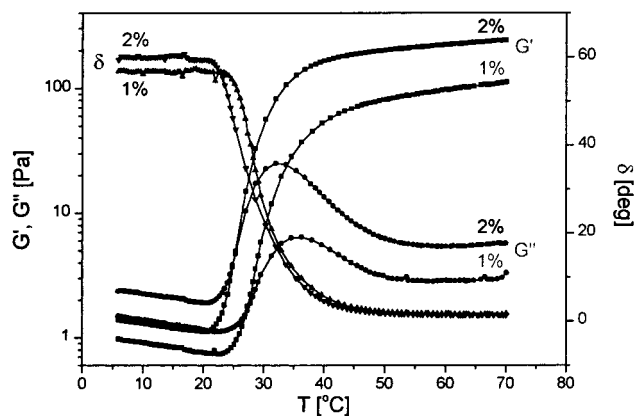


Figure 1. Rheological properties of Pluronic-PAA aqueous solutions. Dynamic moduli (G' , G'') and phase angle of 1 and 2 wt % Pluronic-PAA solutions as a function of temperature, given 1 Hz oscillatory shear frequency and 0.6 Pa oscillatory stress.

phobic PPO cores and hydrated PEO coronae. Through an analysis of the SANS measurements on the Pluronic-PAA solutions, insight has been gained into the structural transitions that occur at the molecular level during temperature-induced gelation.

Experimental Procedure

Materials. Poly(ethylene oxide)-*b*-poly(propylene oxide)-*b*-(poly(ethylene oxide))-*g*-poly(acrylic acid) (CAS# 186810-81-1) was synthesized from Pluronic F127 NF (CAS# 9003-11-6) (Pluronic is a registered trademark of BASF Corp.) by suspension polymerization of acrylic acid along with simultaneous grafting of poly(acrylic acid) onto the Pluronic backbone, as described previously.¹¹ The resulting copolymer, which we will call Pluronic-PAA, has been characterized using NMR, SEC, and FTIR.¹¹ The composition of the neutralized copolymer is 44 wt % Pluronic F127 and 56 wt % poly(sodium acrylate), resulting in an average molecular structure per F127 unit of (EO₁₀₀-PO₆₅-EO₁₀₀)-*g*-AA₁₇₀, with an average molecular weight of 28 550 g/mol per subunit.

Procedures. *Rheological Measurements.* Rheological measurements were conducted at pH 7.0 on Pluronic-PAA aqueous solutions using a controlled-stress Rheolyst series AR1000 rheometer (TA Instruments) with a cone and plate geometry (cone: diameter, 4 cm; angle, 2°, truncation, 57 μm) equipped with a solvent trap. Temperature control was provided by Peltier plates.

SANS Measurements. Small-angle neutron scattering measurements were performed at the NIST Center for Neutron Research in Gaithersburg, MD. Polymer solutions were prepared in D₂O and neutralized to pH 7 by addition of 6 M NaOH (1 vol %). A neutron wavelength of 6 Å with a resolution ($\Delta\lambda/\lambda$) of 0.15 was used to measure scattered intensity for a range of scattering vectors (q) covering the range 0.008–0.10 Å⁻¹. Measurements were performed between 15 and 45 °C with an accuracy of ±0.2 °C. It has been previously established that the isotope effect for the temperature-sensitive micellization of Pluronic copolymers is small, using D₂O instead of H₂O.²² We expect self-association and rheological behavior for solutions of Pluronic-PAA similarly to be independent of the degree of deuteration of the solvent phase.

Results and Discussion

Rheological Measurements. The reversible transition between liquid and gel states for solutions of Pluronic-PAA can be readily characterized by oscillatory shear experiments (Figure 1). At low temperatures, both 1 and 2 wt % solutions demonstrate Newtonian liquidlike behavior with the loss modulus (G'') higher than the storage modulus (G') (Figure 1). As the

temperature is increased, G' increases rapidly by 2 orders of magnitude over a narrow temperature range and becomes larger than G'' . This is coincident with a decrease in the phase angle (δ). Thermal reversibility of the rheological properties has been previously established.^{8,9}

Similar thermally induced gelation has been reported previously only with very concentrated solutions of Pluronic (>16 wt %)^{12,23} and significantly is not observed with physical blends of (nongrafted) PAA and Pluronic of equivalent (low) concentrations such as have been studied here. At elevated temperatures, these concentrated Pluronic solutions yield gel networks consisting of interconnected micelles with entangled PEO segments.^{24,25} The onset of the G' increase serves as an indication of gelation.^{8,9} We note that the gelation point decreases by approximately 2 °C with a doubling of the Pluronic-PAA concentration, which is consistent with the changes in the critical micellization temperature observed for the parent Pluronic F127 copolymer when the concentration is doubled.

SANS Measurements. Measurements of SANS spectra for 1 and 2% solutions of Pluronic-PAA polymer were performed at a number of different temperatures (Figure 2a,b). Several features are apparent from these measurements. There is a clear progression from weak scattering, at the lower temperatures, to stronger scattering, with a well-defined scattering maximum becoming apparent at the higher temperatures (36, 45 °C). For these higher temperature measurements, the position of the peak does not change with temperature but changes approximately with polymer concentration to the one-third power, as would be expected for scattering centers whose sizes are concentration-independent (Figure 2c). For polymer solutions at 15 °C, the scattering signal is much weaker, suggesting that discrete scattering centers have not formed. Similarly, at 25 °C, no clear peak is resolved for 1% solutions, although for 2% solutions the beginnings of a peak are clearly evident, implying progress toward the formation of scattering centers. This is consistent with the decrease in T_{gel} observed rheologically with increasing polymer concentration. Solutions of pure Pluronic copolymers have been studied using SANS^{22,24,26,27} and show a similar increase in scattering intensity with increasing temperature. The appearance of a broad peak above the critical micellization temperature only occurs for more concentrated (5%) solutions and has been modeled with a structure factor for hard-sphere interactions.²² The narrow peaks seen with Pluronic-PAA solutions suggest greater order to the spacing of the scattering centers in these gels than in pure Pluronic micellar solutions.

The formation of scattering centers at the onset of gelation is apparent from an examination of the scattering intensity at sufficiently high q values, where the intensity is dominated by the form factor (representing the size and shape of the scatterers) rather than the structure factor (representing interparticle interactions). Scattering intensity vs temperature at $q = 0.05$ Å⁻¹ (Figure 3) reveals a transition in the same region over which gelation occurs. This agrees with previous dynamic light scattering data,^{2,5,6} which showed an increase in the population of large scatterers upon gelation. The absolute value of T_{gel} and the shift in T_{gel} with concentration of polymer are consistent with the critical micellization temperature (cmt) behavior of Pluronic solutions and the rheological data of Figure 1. Empirical

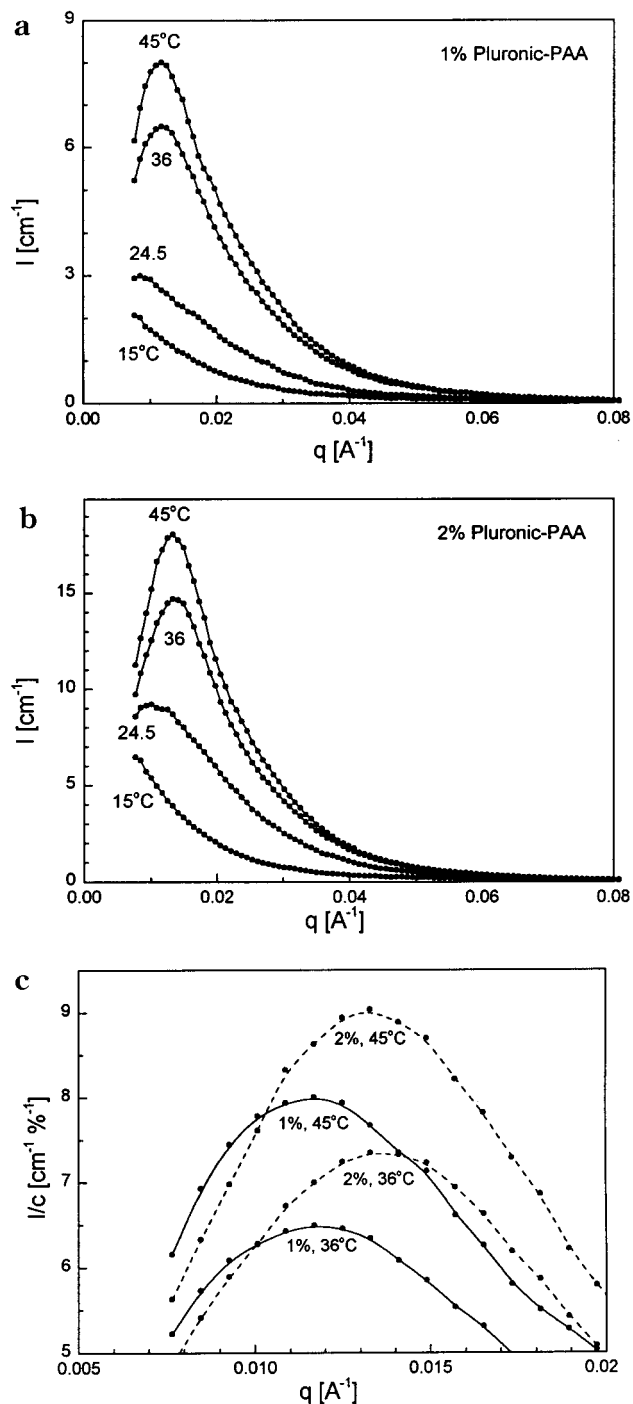


Figure 2. Small-angle neutron scattering data from Pluronic-PAA solutions as a function of temperature for (a) 1% and (b) 2% solutions. (c) Details of the scattering intensity maxima for 1 and 2% solutions at 36 and 45 °C.

formulations²⁸ for the temperature and concentration dependence of micellization properties predict a cmt of 26.4 °C for 0.44 wt % F127 solutions (equivalent to 1.0% Pluronic-PAA solutions) and 24.4 °C for 0.88 wt % F127. Thus, cmt decreases by 2.0 °C for a factor of 2 increase in concentration, and T_{gel} decreases approximately 2 °C with a similar increase.

Direct Model Fitting. Additional structural information can be extracted from the SANS data through direct formulation of a model for the scattering centers in solution. The scattered intensity is a product of the form factor and the structure factor according to the equation

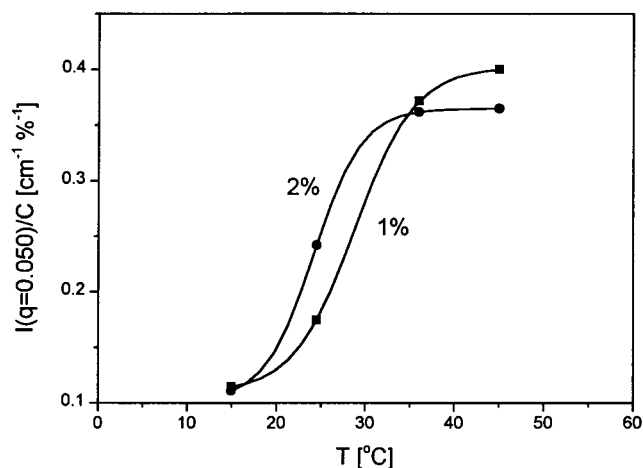


Figure 3. Temperature dependence of neutron scattering at $q = 0.050 \text{ \AA}^{-1}$, representing a regime where scattering is dominated by the particle form factor.

$$I(q) = (\Delta\rho)^2 NP(q) S(q)$$

where N is the number density of scattering centers and $\Delta\rho$ is the contrast difference between the scattering center and the solvent. The form and structure factors are given by $P(q)$ and $S(q)$, respectively. At low q , the structure factor dominates, and the distance between scattering objects (D) can be effectively determined from the position of the intensity peak (q_{max}). The position of q_{max} is given explicitly by a complex function of the micelle radius and volume fraction.²⁹ In the simplifying case of a frozen matrix of noninteracting hard spheres, this can be reduced to the simple equation³⁰

$$D = 2\pi/q_{\text{max}}$$

The results are summarized in Table 1, where, within experimental error, the interparticle distance varies inversely with concentration to the one-third power. This is anticipated since the size of the scattering center structures does not depend on polymer concentration, as confirmed by the form factor data for the particle radii (similar to Pluronic micelles). No temperature dependence of the intensity peak was noted (Figure 2c). From this information, we can estimate the number density, N , of scattering centers. In the higher q range ($q = 0.040\text{--}0.090$) where S approaches unity, the scattering intensity is determined by the form factor, which depends only on the properties of the individual scattering centers. We assume the scattering centers to have the structure of block copolymer micelles.

A standard model for triblock copolymer micelles is the core-corona model, where the scattering center is composed of a spherical core of one scattering length density (SLD), surrounded by a corona of some other SLD. The SLDs of the two regions are determined by their respective polymer compositions and degrees of hydration.^{22,24,31} Goldmints et al.²² showed that such a model cannot be used to determine simultaneously the core and corona radii, and their respective degrees of hydration, without ambiguity. The corona hydration level can be derived by material balance knowing the two radii and assuming that all PEO blocks associated with the PPO in the core are included in the corona. If the core hydration is specified, then the number of model parameters is reduced to two, the core and corona radii, and these can be determined uniquely from the

Table 1. SANS-Derived Parameters for the Scattering Centers of the Pluronic–PAA Solution in the Gel State (36 and 45 °C), Including Distance between Centers (D), Core and Corona Radii, Hydration Level of Corona, and Fraction of Pluronic Present in Scattering Centers^a

C [wt %]	q_{\max} [\AA^{-1}]	D [\AA]	R_{core} [\AA]	R_{corona} [\AA]	% corona hydration	% PPO in core
1.0	0.011 68	540 ± 20	26.8 ± 0.3	59.5 ± 1.2	78.5	39.0
2.0	0.013 29	470 ± 15	27.9 ± 0.2	59.3 ± 0.7	75.6	33.2

^a Error estimates in D are one-half the distance between data points (calculated from the q data spacing); radii error estimates are model fitting results.

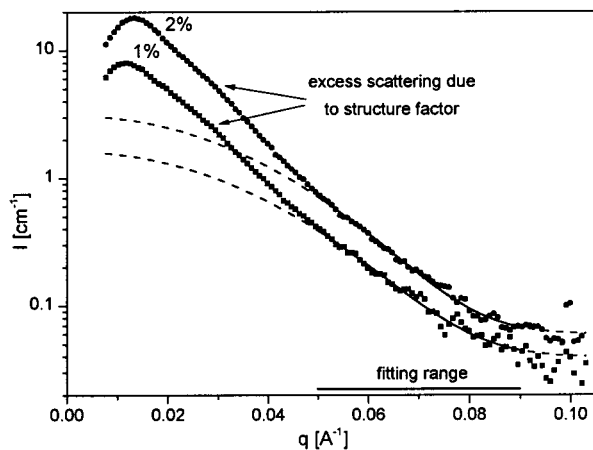


Figure 4. Core–corona model fits to small-angle neutron scattering data from Pluronic–PAA polymer solutions for 1% and 2% solutions at 45 °C. Models assuming a dehydrated core and models for other degrees of hydration give essentially identical fits.

SANS results under the imposed constraints. Goldmints et al.^{22,27} also showed that above the transition region the level of hydration of the PPO cores in block copolymer micelles is at most 20%. We have, therefore, analyzed the SANS spectra using the model of a PPO core of specified degree of hydration surrounded by a corona of hydrated PEO to obtain estimates of the core and corona radii as functions of the core hydration level. These calculations provided bounds on the actual values of the micelle structural parameters.

The particle form factor function for the core–corona model is given by²²

$$P(q)(\Delta\rho)^2 = (4\pi/q^3)^2 [(\rho_1 - \rho_2)(\sin(qR_1) - qR_1 \cos(qR_1)) + (\rho_2 - \rho_s)(\sin(qR_2) - qR_2 \cos(qR_2))]^2$$

where ρ_1 , ρ_2 , and ρ_s are the scattering length densities for core, corona, and solvent, respectively; R_1 is the core radius and R_2 the corona radius. Scattering length densities are calculated for the different species as 6.38×10^{-6} (D_2O), 0.59×10^{-6} (PEO), 0.33×10^{-6} (PPO), and $2.66 \times 10^{-6} \text{\AA}^{-2}$ (PAA^+Na^-).³² The scattering data were corrected for scattering from the solvent, the quartz cell, and background. This model was fitted to scattering over the q range of 0.04–0.09 \AA^{-1} , where form factor contributions dominate, and $S(q)$ can be reasonably assumed to be unity.

The resulting core–corona model fits for a dehydrated PPO core are shown in Figure 4 for the two polymer concentrations at a temperature of 45 °C. These fits are essentially indistinguishable from those obtained assuming a 20% hydration of the core, although, of course, the extracted parameter values do differ somewhat. The

change in model parameters in going from a dehydrated core to a core hydration of 20% was slight; the core radius increased by 7%, the corona radius fell by 4%, and the corona hydration decreased by 3%, while the fraction of the total Pluronic participating in the core fell by 3%. These results provide sufficiently narrow bounds on the micelle core and corona sizes and hydration levels that we can draw realistic conclusions on the structure of the aggregates from them.

An analysis of the core–corona model fit for dehydrated cores reveals a core radius of 28 \AA , a corona radius of 59 \AA , and corona hydration of 78%, independent of polymer concentration (Table 1). A simple mass balance can be calculated, comparing the PPO polymer participating in the scattering center cores to the total PPO polymer in solution. On the basis of these values, it can be estimated that approximately one-third (33–39%) of the Pluronic present in the polymer solution participates in the scattering centers. The rest must reside in the space between scattering centers. This is consistent with the known characteristics of the grafting process in the polymer synthesis. It may be reasonably assumed that grafting of the PAA to the PPO block of the Pluronic will prevent that Pluronic copolymer from participating in the formation of the scattering centers, as the ability of a PPO block to dehydrate and collapse into a dehydrated core with other PPO blocks may be disrupted by the PAA. A graft of PAA to PPO is several times (3–8 times) more likely than a graft to PEO, given the nature of the grafting initiation through hydrogen abstraction.⁹ PPO represents only 30% of the Pluronic F127 molecule, so given a low number of grafts per molecule and 5 times preference for PPO grafting, it can be estimated that about 68% of the Pluronic has grafts attached to the PPO blocks, the remainder having been grafted to the PEO blocks. It is reasonable to expect these Pluronic molecules to have a reduced tendency to aggregate with increasing temperature because of the hydration of the attached PAA. From this rough calculation we would estimate that only 32% of the Pluronic polymers would incorporate into the micelle-like scattering centers, with the remaining Pluronic in the space between centers.

Nature of Pluronic–PAA Hydrogel. The thermally reversible character of the Pluronic–PAA system can be attributed to its chemical composition and unique block–graft arrangement, resulting in a material with novel physical properties. The entropy-driven aggregation of the PPO blocks (representing 13 wt % of the copolymer) at elevated temperatures is responsible for the reversible gelation behavior of the material, as these aggregates serve to cross-link the polymer and cause a gel. The role of the PAA component grafted to the Pluronic is to provide a highly water-absorbing matrix when the ionizing groups are neutralized to a pH above their pK_a . The remaining space not taken by PEO–PPO–PEO aggregates is occupied by PAA. Cross-linked neutralized PAA has been widely studied and developed as a super-absorbent material for a variety of personal care products. It is well-known that cross-linked PAA can create a hydrogel absorbing up to 100 times its own weight of water,³³ a level of hydration consistent with the proposed model (Figure 5).

For most temperature-responsive materials, one common aspect is the change from an expanded to a collapsed state of the polymer in solution as the temperature is raised through the gelation threshold, ac-

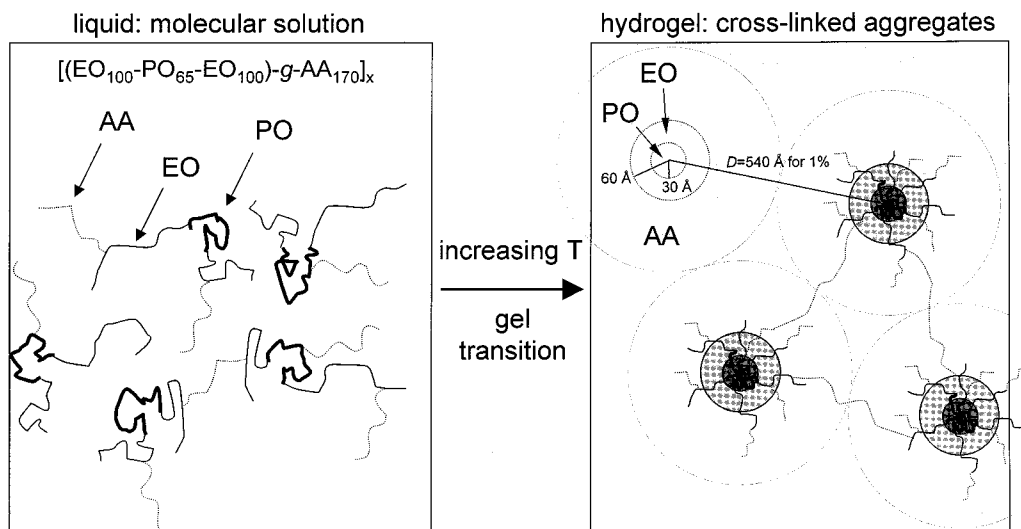


Figure 5. Scheme of Pluronic-PAA polymer organization in solution above and below the critical micellization temperature corresponding to the gelation threshold. Gelation occurs due to network formation caused by cross-linking of scattering centers that form by the dehydration and physical association of the PPO blocks, as the temperature is increased. As a typical Pluronic-PAA molecule contains more than one Pluronic subunit, some physical PAA cross-linking exists between the dehydrated cores. The PAA chains cross-linking the aggregates serve as junctions, yielding gels as described by the Scanlan-Case criterion.¹⁰ Transient rheological characteristics and dynamics of the Pluronic-PAA hydrogels have been discussed previously.^{8,10}

accompanied by a visible phase separation of the polymer, as with poly(*N*-isopropylacrylamide) (pNIPAA).^{34,35} Such behavior can also occur through increased electrolyte strength, as reported by Hourdet et al. for salt-induced thickening of aqueous solutions of (PAA-*g*-PEO) copolymers,³⁶ where salting-out effects cause phase separation of the PEO side chains which then serve as cross-links in the ensuing physical gels. In contrast, an unusual feature of the Pluronic-PAA material is that it maintains an expanded state both above and below T_{gel} and undergoes no visible phase separation. The temperature-sensitive component of other hydrogel polymers forces a change in gel structure with temperature above the lower critical solution temperature (LCST), as macroscopic phase separation occurs (for example, the phase separation pNIPAA above 32 °C). In contrast, the aggregation of the PPO block of the Pluronic-PAA polymer into micelle-like dehydrated cores of 30 Å radius does not cause a macroscopic phase separation.⁷

Conclusion

The unique block-graft structure (A-B-A)-*g*-C of the Pluronic-PAA copolymer leads to reversible formation of a hydrogel without phase separation as the temperature is raised above T_{gel} , for 1–2% solutions. The transition between the liquid and gel states is clearly detected using rheological measurements and small-angle neutron scattering (SANS). From the position of the intensity peak in the scattering profile of the gel state, a characteristic distance between scattering centers is determined to be of the order of 50 nm. This peak in intensity is much better defined than would be expected for randomly tethered scattering centers. This observation is consistent with a space-filling model of uniformly spaced micelle-like aggregates consisting of a mostly dehydrated poly(propylene oxide) core, followed by a hydrated poly(ethylene oxide) corona. The remaining volume is essentially filled with highly hydrated and branched poly(sodium acrylate), and the PEO-PPO-PEO triblock copolymer not participating in the scattering centers. The size of these centers is almost

concentration independent, as would be expected for micelle-like aggregates.

Acknowledgment. This work was partially supported by a grant from Gel Sciences Inc., Bedford, MA. This work is based upon activities supported by the National Science Foundation under Agreement DMR-9423101. We acknowledge the support of the National Institute of Standards and Technology, U.S. Department of Commerce, in providing the neutron research facilities. The assistance of Dr. Steven Kline at NIST is greatly appreciated. L.E.B. is grateful to Professor Michael Rubinstein and Professor Toyochi Tanaka for insightful discussions.

References and Notes

- (1) Bromberg, L.; Lupton, E. C.; Schiller, M. E.; Timm, M. J.; McKinney, G. W.; Orkisz, M.; Hand, B. *Int. Pat. Appl. WO 97/00275*, 1997.
- (2) Bromberg, L.; Orkisz, M.; Roos, E.; Ron, E. S.; Schiller, M. *J. Controlled Release* **1997**, *48*, 305–308.
- (3) Bromberg, L. E.; Mendum, T. H. E.; Orkisz, M. J.; Lupton, E. C.; Ron, E. S. *Polym. Prepr.* **1997**, *38*, 602–603.
- (4) Bromberg, L. E.; Orkisz, M. J.; Ron, E. S. *Polym. Prepr.* **1997**, *38*, 626–627.
- (5) Bromberg, L. *J. Phys. Chem. B* **1998**, *102*, 1956–1963.
- (6) Bromberg, L. E.; Ron, E. S. *Adv. Drug Delivery Rev.* **1998**, *31*, 197–221.
- (7) Bromberg, L. E.; Goldfeld, M. G. *Polym. Prepr.* **1998**, *39*, 681–682.
- (8) Bromberg, L. *Macromolecules* **1998**, *31*, 6148–6156.
- (9) Bromberg, L. *J. Phys. Chem. B* **1998**, *102*, 10736–10744.
- (10) Bromberg, L. *Langmuir* **1998**, *14*, 5806–5812.
- (11) Bromberg, L. *Ind. Eng. Chem. Res.* **1998**, *37*, 4267–4274.
- (12) Alexandridis, P.; Hatton, T. A. *Colloids Surf. A* **1995**, *96*, 1–46.
- (13) Bastide, J.; Candau, S. J. In *Physical Properties of Polymeric Gels*; Cohen Addad, J. P., Ed.; Wiley: New York, 1996.
- (14) Horkay, F.; Hecht, A.-M.; Geissler, E. *Macromolecules* **1994**, *27*, 1795–1798.
- (15) Kanaya, T.; Ohkura, M.; Kaji, K.; Furusaka, M.; Misawa, M.; Yamaoka, H.; Wignall, G. D. *Physica B: Condens. Matter* **1992**, *180*, 549–551.
- (16) Kanaya, T.; Ohkura, M.; Kaji, K.; Furusaka, M. *Macromolecules* **1994**, *27*, 5609–5615.

- (17) Krueger, S.; Andrews, A. P.; Nossal, R. *Biophys. Chem.* **1994**, *53*, 85–94.
- (18) Renard, D.; Axelos, M. A. V.; Boue, F.; Lefebvre, J. *J. Chim. Phys. Phys.-Chim. Biol.* **1996**, *93*, 998–1015.
- (19) Shibayama, M.; Tanaka, T.; Han, C. C. *J. Chem. Phys.* **1992**, *97*, 6829–6841.
- (20) Shibayama, M.; Tanaka, T.; Han, C. C. *J. Chem. Phys.* **1992**, *97*, 6842–6854.
- (21) Ikkai, F.; Shibayama, M.; Han, C. C. *Macromolecules* **1998**, *31*, 3275–3281.
- (22) Goldmints, I.; von Gottberg, F. K.; Smith, K. A.; Hatton, T. A. *Langmuir* **1997**, *13*, 3659–3664.
- (23) Malmsten, M.; Lindman, B. *Macromolecules* **1992**, *25*, 5440–5445.
- (24) Mortensen, K.; Pedersen, J. S. *Macromolecules* **1993**, *26*, 805–812.
- (25) Mortensen, K.; Brown, W.; Jørgensen, E. *Macromolecules* **1994**, *27*, 5654.
- (26) Wu, G.; Chu, B.; Schneider, D. K. *J. Phys. Chem.* **1995**, *99*, 5094–5101.
- (27) Goldmints, I.; Yu, G.-E.; Booth, C.; Smith, K. A.; Hatton, T. A. *Langmuir* **1999**, *15*, 1651–1656.
- (28) Alexandridis, P.; Holzwarth, J. F.; Hatton, T. A. *J. Am. Oil Chem. Soc.* **1995**, *72*, 823–826.
- (29) Mortensen, K. *J. Phys.: Condens. Matter* **1996**, *8*, A103–A124.
- (30) Steytler, D. C.; Robinson, B. H.; Eastoe, J.; MacDonald, I. In *Micelles, Microemulsions, and Monolayers: Science and Technology*; Shah, D. O., Ed.; Marcel Dekker: New York, 1998.
- (31) Glatter, O.; Scherf, G.; Schillen, K.; Brown, W. *Macromolecules* **1994**, *27*, 6046–6054.
- (32) Sears, V. F. *Neutron News* **1992**, *3*, 26–37.
- (33) Buchholz, F. L. In *Superabsorbent Polymers: Science and Technology*; Buchholz, F. L., Peppas, N. A., Eds.; American Chemical Society: Washington, DC, 1994.
- (34) Chen, G.; Hoffman, A. S. *Macromol. Chem. Phys.* **1995**, *196*, 1251–1259.
- (35) Brazel, C. S.; Peppas, N. A. *Macromolecules* **1995**, *28*, 8016–8020.
- (36) Hourdet, D.; L'alloret, F.; Durand, A.; Lafuma, F.; Audebert, R.; Cotton, J.-P. *Macromolecules* **1998**, *31*, 5323–5335.

MA990181T